

Position/Attitude Control of an Object by Controlling a Fluid Field Using a Grid Pattern Air Nozzle

Takeshi Takaki, Satomi Tanaka, Tadayoshi Aoyama and Idaku Ishii

Abstract—A manipulator which enables noncontact control of the position and attitude of an object on a plane by controlling a fluid field is proposed. The manipulator comprises 2 boards with grid pattern arrangements of holes and a parallel link robot which is capable of translational motion with 2 degrees of freedom and rotational motion with 1 degree of freedom in a plane. Air jets are discharged from the grid of holes. The direction of the air jets from the holes can be controlled by changing the positional relationship of the 2 boards by means of the parallel link robot. This makes it possible to form an air flow with a unidirectional fluid field or a vortex-like fluid field. When an object is placed in the fluid field, translational motion and rotational motion of the object are possible. If the position and attitude of the object are photographed and calculated using high speed camera and feedback control is performed, the position and attitude of the object can be controlled. The structure of the manipulator and the principle of control of the fluid field are described, and the possibility of controlling the translational motion and rotational motion of an object is demonstrated experimentally.

I. INTRODUCTION

In general, when a manipulator is used to manipulate an object, the manipulator comes into physical contact with the object. In virtually all cases, both the manipulator and the object are solids. Technologies for manipulation of objects by contact between solid bodies are widely used at production sites and have made an important contribution to the progress of industry. On the other hand, with the aim of improving manipulation technology, techniques which realize manipulation without contact between solids have been reported, by methods utilizing air jets, electromagnetism, sonic wave, and the like. If solids do not come into contact, problems due to impact, wear, etc. can be alleviated, and will become possible to apply robotic manipulation techniques of a wider range of objects.

This paper proposes a technology for noncontact manipulation of the position and attitude of an object on a plane,

focusing on air jets, which can be handled with comparative ease and are capable of outputting comparatively large force. Previously, a method for manipulating an object by applying air jets from several points was proposed [1]-[3]. In this case, it is assumed hypothetically that the air impinges on the object at a point, as illustrated in Fig. 1(a). However, an air jet spreads after discharge from a nozzle, and mutual interference between air jets occurs when multiple jets are used, making it difficult to grasp the flow of the air entirely. It is thought that these problems can be alleviated if the fluid field of air surrounding the object can be controlled, as shown in Fig. 1(b), and as a result, the object can be manipulated with greater precision. Therefore, in this paper, a manipulator which makes it possible to control the fluid field is proposed. The proposed manipulator comprises 2 boards with grid pattern arrangements of openings and a parallel link robot which enables translational motion with 2 degrees of freedom and rotational motion with 1 degree of freedom in a plane.

As a conventional method for manipulating objects by using air, a noncontact method in which the translational motion of a spherical object is controlled with 3 degrees of freedom in space by an air jet discharged from a nozzle whose direction can be manipulated freely was proposed [4]. However, with that method, it is difficult to control the attitude of the object and manipulate the object in a plane. Consequently, the applications in which it can be used are different from the method proposed here. Although numerous other methods of manipulating objects by using air have also been reported, these are techniques for moving an object only in a designated direction [5][6] and techniques for suction-type transportation [7][8]. A technique which uses air jets to give a sense of a virtual object has also been reported, but this is not a technique for manipulating the motion of an object [9].

Chapter II describes the structure of the 2 boards which comprise the proposed manipulator and the principle of operation in which translational motion and rotational motion of an object is realized by blowing air from the holes in those boards. The structure of a parallel link robot for manipulating these boards and the overall structure of the proposed manipulator are also described. Chapter III proposes a control method for manipulating the translational motion and rotational motion of an object by acquiring the position and attitude of the object by high speed camera and performing feedback control. Chapter IV describes a prototype manipulator which was actually fabricated. Chapter V presents an experimental demonstration that control of the

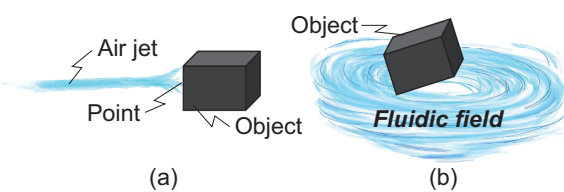


Fig. 1. Concept of proposed technique

T. Takaki, S. Tanaka, T. Aoyama, and I. Ishii are with the Department of System Cybernetics, Graduate School of Engineering Hiroshima University, Hiroshima 739-8527, Japan. takaki@robotics.hiroshima-u.ac.jp

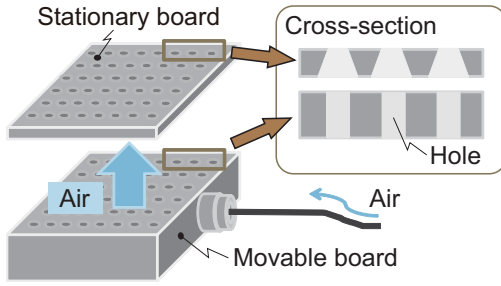


Fig. 2. Structure of stationary board and movable board (manipulator)

translational motion and rotational motion of an object is possible. Chapter VI summarizes the contents of the paper.

II. STRUCTURE OF MANIPULATOR AND PRINCIPLE OF OPERATION

The proposed manipulator which enables translational/rotational motion of an object on a plane comprises 2 boards and a parallel link robot. Section II-A describes the configuration of the 2 boards, II-B outlines the principle of operation for translational/rotational motion of an object, II-C discusses the parallel link robot, and II-D describes the overall structure of the manipulator.

A. Structures of 2 boards

The structures of the 2 boards are shown in Fig. 2. Because the lower board can be moved relative to the upper board, the upper board is called the "stationary board" and the lower board is called the "movable board." The stationary board has a grid pattern arrangement of truncated conical holes, and the movable board has a similar arrangement of cylindrical holes.

B. Principle of operation

As shown in Fig. 3, an object is placed on the stationary board, and air jets are discharged from below. When there is no deviation between the positions of the holes on the 2 boards, the airflow is perpendicular with respect to the boards, as in Fig. 3(a). In this case, the object is lifted slightly, but horizontal translational motion and rotational motion do not occur. On the other hand, if the positions of the board are offset, as shown in Fig. 3(b), the direction of the airflow becomes inclined. In this case, the object receives horizontal force, and translational motion and rotational motion are realized by using this force.

When the movable board is moved translationally in the direction of the arrow in Fig. 4(a) without rotation, the direction of the airflow becomes unidirectional and the object undergoes translational motion. However, if the movable board is rotated as shown in Fig. 4(b), the airflow forms a vortex, which causes rotational motion of the object.

C. Parallel link robot

The parallel link robot shown in Fig. 5(a) is used to manipulate the movable board. This robot has 3 sliders that move rectilinearly. The 3 sliders and the end-effector are

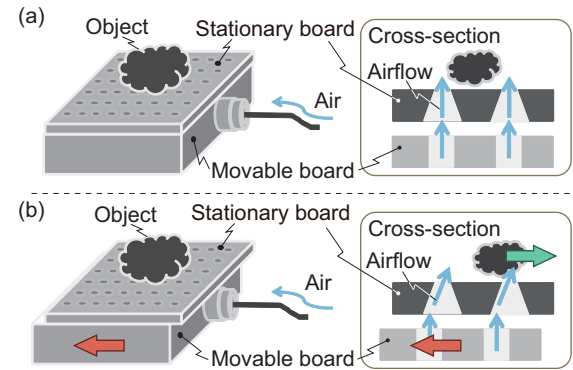


Fig. 3. Principle of formation of fluid field

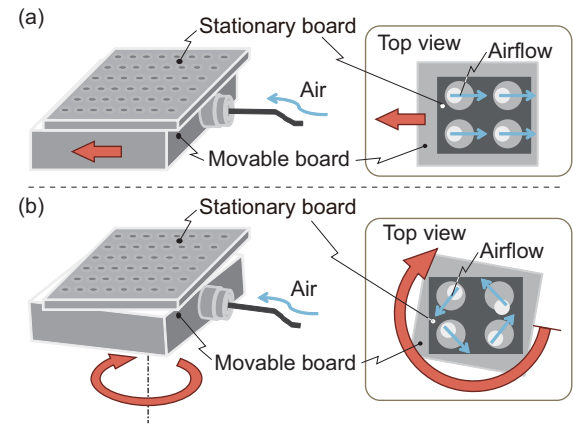


Fig. 4. Fluid fields for (a) translational motion and (b) rotational motion

connected by links. Translation of the end-effector in the directions of the x - and y -axes and rotation of the effector in the θ direction are possible by driving the sliders.

D. Overall structure

As illustrated in Fig. 5(b), the movable board is attached to the end-effector, and the stationary board is fixed. Based on the principle of operation described in section II-B, translational motion of an object in the directions of the x - and y -axes and rotational motion in the θ direction are realized by using the parallel link robot to manipulate the movable board.

III. CONTROL METHOD

The flow of control for controlling an object to a desired position/attitude P_d is shown in Fig. 6. In section III-A, the object is photographed with a high speed camera, and the position/attitude P_o of the object are calculated by image processing. In section III-B, the position/attitude P_{dm} to which the movable board should be moved in order to move the position/attitude P_o of the object to the desired position/attitude P_d is determined. In section III-C, the desired movement distance s_{dj} of the sliders for driving the end-effector of the parallel link robot to the desired position/attitude P_{dm} is obtained by inverse kinematics. In

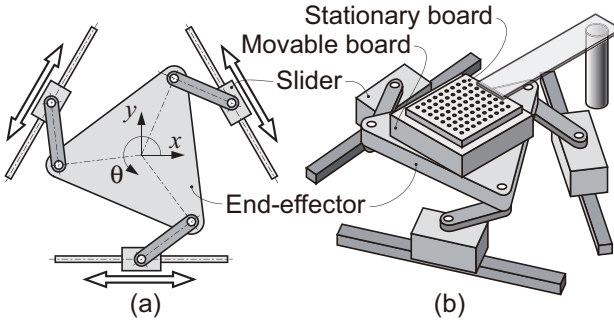


Fig. 5. Structure of manipulator

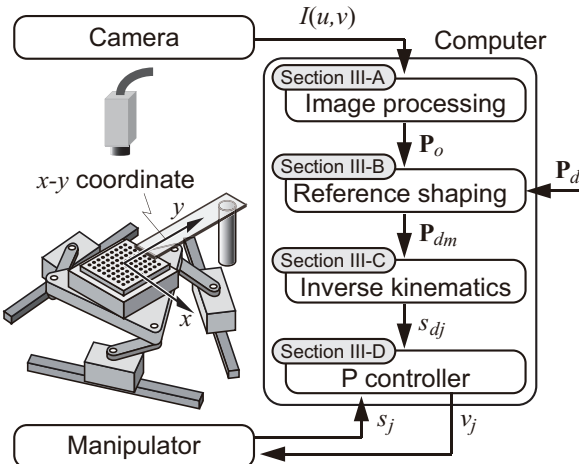


Fig. 6. Schematic diagram of the system

section III-D, a method for controlling the respective sliders to the desired movement distance s_{dj} using P control is described.

A. Image processing

The u and v axes of the image photographed by the high speed camera are defined as shown in Fig. 7. The size of the image is defined as (U, V) , and the brightness of the pixel at position (u, v) is defined as $I(u, v)$. Two markers are attached to the object, and the position/attitude of the object $\mathbf{P}_o = [x_o, y_o, \theta_o]$ is calculated by recognition of those markers on the image. The brightness of the pixel where the markers are photographed is assumed to be larger than that of the other pixels. At this time, the markers can be extracted if the image is binarized by using a threshold value θ_{th} . The binarized image $I_b(u, v)$ is obtained from the following Eq. (1).

$$I_b(u, v) = \begin{cases} 1 & I(u, v) \geq \theta_{th} \\ 0 & I(u, v) < \theta_{th} \end{cases} \quad (1)$$

The moment m_{pq} of the p^{th} image on the u -axis direction and the q^{th} image in the v -axis direction is given by Eq. (2).

$$m_{pq} = \sum_{u=0}^{U-1} \sum_{v=0}^{V-1} u^p v^q I_b(u, v) \quad (2)$$

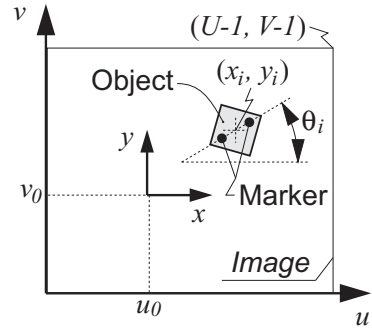


Fig. 7. Coordinates of image and position/attitude of object

The position/attitude of the object on the image $[u_i, v_i, \theta_i]$ is given by Eq. (3).

$$[u_i, v_i, \theta_i] = \left[\frac{m_{10}}{m_{00}}, \frac{m_{01}}{m_{00}}, \frac{1}{2} \tan^{-1} \left(\frac{2m_{11}}{m_{20} - m_{02}} \right) \right] \quad (3)$$

The x - y coordinates on the stationary board are defined as shown in Fig. 6. Furthermore, the x - y coordinates are assumed to be offset $[u_0, v_0]$ on the screen, as shown in Fig. 7. In case 1 pixel is equivalent to length l , the position/attitude of the object \mathbf{P}_o is obtained from Eq. (4).

$$\mathbf{P}_o = [l(u_i - u_0), l(v_i - v_0), \theta_i] \quad (4)$$

B. Desired position/attitude of movable board

This section considers how the movable board should be moved in order to control an object to a desired position/attitude $\mathbf{P}_d = [x_d, y_d, \theta_d]$. In this section, the desired position/attitude of the moveable board $\mathbf{P}_{dm} = [x_{dm}, y_{dm}, \theta_{dm}]$ is determined by \mathbf{P}_o and \mathbf{P}_d . For simplicity, it is assumed that superposition of the operations in Fig. 4(a) and (b) is materialized in the case of simultaneous translational motion and rotational motion of an object. That is, assuming that the component which causes translational motion of the object is $\mathbf{T} = [x_{dmt}, y_{dmt}, \theta_{dmt}]$ and the component which causes rotational motion is $\mathbf{R} = [x_{dmr}, y_{dmr}, \theta_{dmr}]$, the following Eq. (5) is assumed to hold.

$$\mathbf{P}_{dm} = \mathbf{T} + \mathbf{R} \quad (5)$$

Translational motion: Here, we will consider the method for translational motion of an object. If translational movement of the movable board is possible, as shown in Fig. 4(a), force can be applied to an object in the translational direction. Therefore, adapting the PD control law, the following two Eqs. (6) and (7) were assumed for the desired position of the movable board $[x_{dmt}, y_{dmt}]$, respectively:

$$x_{dmt} = g_1(x_o - x_d) + g_2 \dot{x}_o \quad (6)$$

$$y_{dmt} = g_1(y_o - y_d) + g_2 \dot{y}_o \quad (7)$$

Where, g_1 and g_2 are proportional gain and derivative gain, respectively. Further, because it is not necessary to rotate the

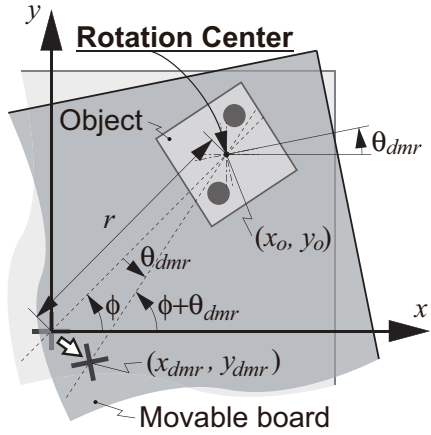


Fig. 8. Relationship of rotation center and position/attitude of movable board

movable board in order to cause translational motion of the object, the desired attitude θ_{dmr} is assumed to be zero:

$$\theta_{dmr} = 0 \quad (8)$$

Rotational motion: Here, we consider the method for rotational motion of the object. If the movable board is rotated around the center of an object as shown in Fig. 4(b), a vortex will be generated, and torque can be applied to the object. First, adapting the PD control law, the following Eq. (9) was assumed for the desired attitude of the movable board θ_{dmr} .

$$\theta_{dmr} = g_3(\theta_o - \theta_d) + g_4\dot{\theta}_o \quad (9)$$

Where, g_3 and g_4 are proportional gain and derivative gain, respectively. Moreover, because the movable board is rotated around the center of the object to the desired attitude θ_{dmr} , this operation is also accompanied by translational motion, as illustrated in Fig. 8. At this time, the desired position $[x_{dmr}, y_{dmr}]$ for translation of the movable board is given by Eqs. (10) and (11).

$$x_{dmr} = x_o - r \cos(\phi + \theta_{dmr}) \quad (10)$$

$$y_{dmr} = y_o - r \sin(\phi + \theta_{dmr}) \quad (11)$$

Where, r is the distance from the origin to the object, and ϕ is the angle between a straight line joining the origin and the object and the x -axis. r and ϕ are given by Eqs. (12) and (13), respectively.

$$r = \sqrt{x_o^2 + y_o^2} \quad (12)$$

$$\phi = \text{Atan2}(y_o, x_o) \quad (13)$$

Where, Atan2 is the arc tangent of the two variables.

As described above, the desired position/attitude of the movable board \mathbf{P}_{dm} is determined by substituting Eq. (6)-(11) into Eq. (5).

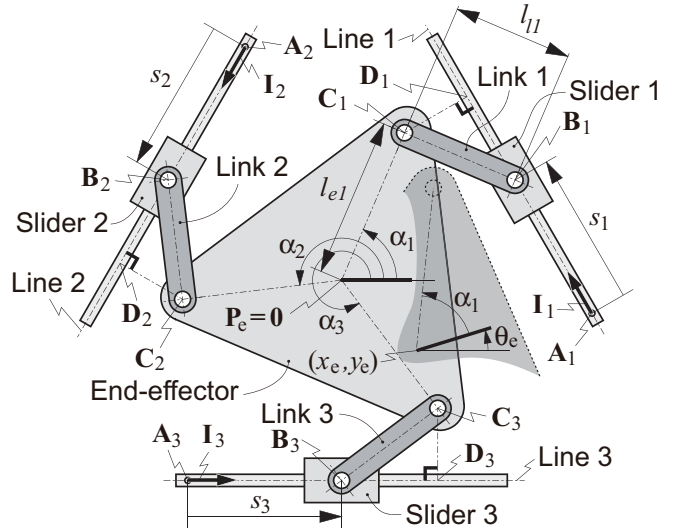


Fig. 9. Parallel link robot

C. Inverse kinematics and desired movement distance of sliders

Positional relationship of component elements: The three sliders are assigned the numbers 1-3, respectively, as shown in Fig. 9. The same numbers are also used for the component elements related to the respective sliders. Slider j ($j = 1, 2, 3$) moves on line j through the reference point $A_j \in \mathbb{R}^2$ in the same direction as the unit vector $I_j \in \mathbb{R}^2$. Assuming the distance from reference point A_j to slider j is s_j , the position of the slider $B_j \in \mathbb{R}^2$ is given by Eq. (14).

$$B_j = A_j + s_j I_j \quad (14)$$

The position/attitude of the center of the end-effector is expressed by $P_e = [x_e, y_e, \theta_e]$. The end-effector is connected with link j at a point distant l_{ej} from this position, and that position is expressed by $C_j \in \mathbb{R}^2$. When $P_e = 0$, the slope of the line joining the origin and position C_j is expressed by α_j . From the above, position C_j is given by Eq. (15).

$$C_j = [x_e + l_{ej} \cos(\theta_e + \alpha_j), y_e + l_{ej} \sin(\theta_e + \alpha_j)] \quad (15)$$

Inverse kinematics: The movement distance of the slider s_j is obtained from the position/attitude of the center of the end-effector P_e . The length of link j joining position B_j and position C_j is l_{lj} . The position of the foot of a perpendicular line from position C_j to line j is $D_j \in \mathbb{R}^2$. The distances from positions A_j , B_j , and C_j to position D_j are l_{ADj} , l_{BDj} , and l_{CDj} , respectively, and are given by the following Eqs. (16)-(18).

$$l_{ADj} = (C_j - A_j) \cdot I_j \quad (16)$$

$$l_{BDj} = \sqrt{l_{lj}^2 - l_{CDj}^2} \quad (17)$$

$$l_{CDj} = (C_j - A_j) \otimes I_j \quad (18)$$

Where $[a, b] \cdot [c, d] = ac + bd$, and $[a, b] \otimes [c, d] = ad - bc$. Accordingly, the slider movement distance s_j is given by Eq.

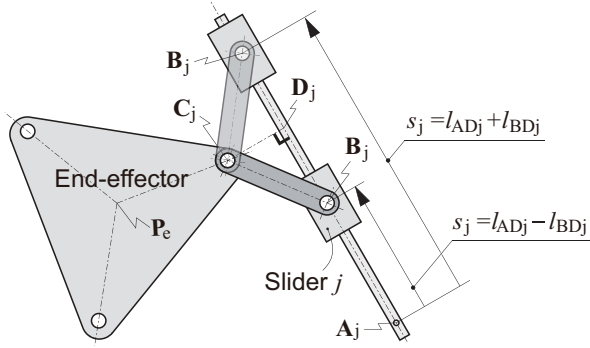


Fig. 10. Two possible solutions

(19).

$$s_j = l_{ADj} \pm l_{BDj} \quad (19)$$

Because two states are possible, two solutions exist, as shown in Fig. 10. However, this does not become a problem, since only one of these states is used and the number of solutions for practical use is determined as one.

Desired movement distance of slider: Since the movable board is fixed to the end-effector, it moves with the effector. In other words, the slider movement distance s_j which is obtained by substituting $\mathbf{P}_e = \mathbf{P}_{dm}$ into Eqs. (14)-(19) becomes the desired movement distance s_{dj} .

D. Control of sliders

This section describes the method for moving slider j to the desired movement distance s_{dj} . The sliders are driven by driving ball screws with motors. The rotation angle of the motors is measured by a rotary encoder, and s_j is obtained from the measured values. The voltage applied to the motor that drives slider j is v_j . The size of the voltage when the motor begins moving from a stationary condition is v_{bias} . Considering the P control law and v_{bias} , voltage v_j was expressed by Eq. (20).

$$v_j = g_5(s_{dj} - s_j) + v_{bias}\text{sgn}(s_j) \quad (20)$$

Where g_5 is proportional gain, and the values of $\text{sgn}(x)$ are as shown in Eq. (21).

$$\text{sgn}(x) = \begin{cases} -1 & x < 0 \\ 0 & x = 0 \\ 1 & x > 0 \end{cases} \quad (21)$$

IV. PROTOTYPE MANIPULATOR AND EXPERIMENTAL SETUP

A stationary board and movable board were fabricated as shown in Fig. 11. The horizontal and vertical dimensions of the two boards are 70 mm each, and the total thickness of the two boards is 19 mm. The boards have a grid pattern arrangement of holes, comprising 15 vertical rows of holes and 15 horizontal rows of holes. The spacing of the holes is 3.5 mm in both vertical and horizontal rows. The holes of the stationary board were machined with a center drill having a diameter of 3 mm. Because a center drill with an

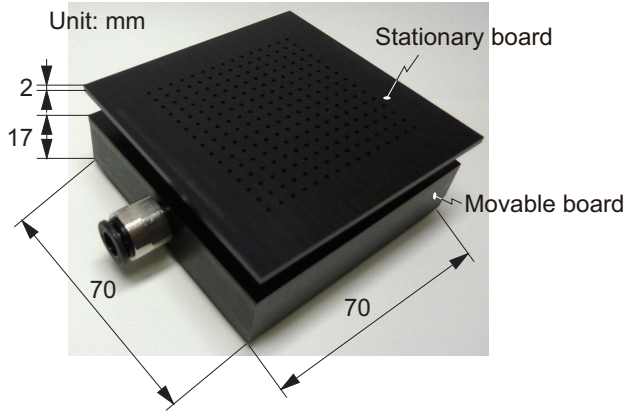


Fig. 11. Prototype stationary board and movable board

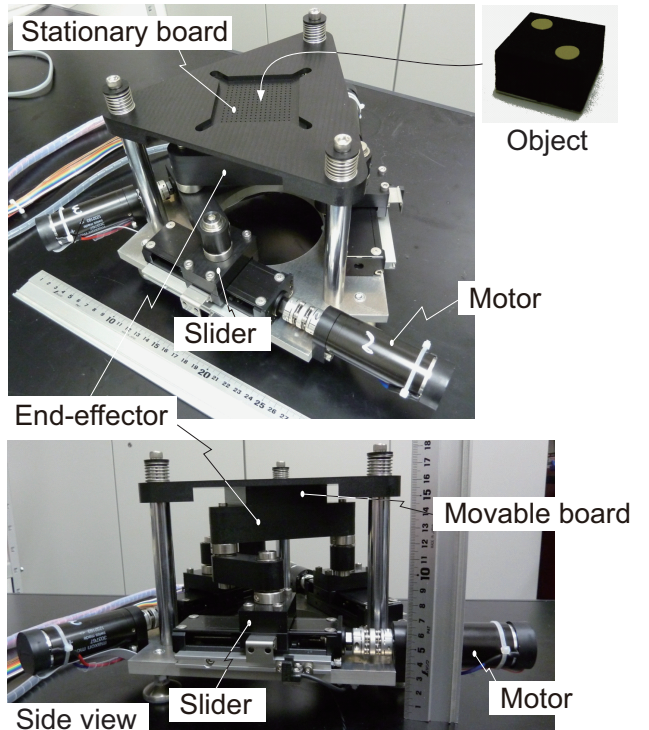


Fig. 12. Experimental setup

edge angle of 90 deg was used, the inclination of the holes with the truncated conical shape is 45 deg relative to the vertical plane. The size of the holes of the movable board is 0.6 mm. The material of the boards is polyacetal.

The movable board was attached to the end-effector of the parallel link robot as shown in Fig. 12, and the stationary board was fixed so as to prevent movement. The motors used to drive the parallel link robot were model RE30 units manufactured by Maxon. The output shaft of the motor is connected to the input shaft of the ball screw that drives the slider. The pitch of the ball screws is 1 mm. The link length l_l is 45 mm. Line j is a tangent of a circle having a radius of 75 mm, and the tangent points are positioned at 3 equidistant points on the circumference. Positions C_j are

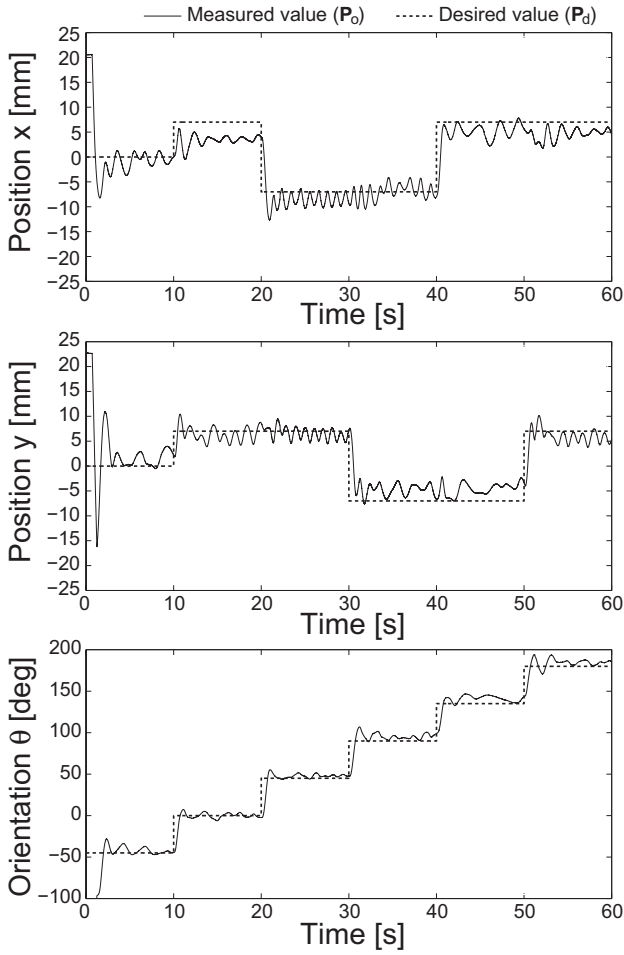


Fig. 13. Position/attitude of object $\mathbf{P}_o = [x_o, y_o, \theta_o]$ and desired position/attitude $\mathbf{P}_d = [x_d, y_d, \theta_d]$

positioned at 3 equidistant points on a circle having a radius $l_l = 60$ mm from the center of the end-effector. The object which was manipulated was a rectangular solid with a length of 20 mm, width of 20 mm, and thickness of 10 mm, and weighed 1.0 g.

The high speed camera used to measure the position/attitude \mathbf{P}_o of the object was an IDP-Express manufactured by Photron. Moment calculations in image processing were performed using a dedicated FPGA image processing board. The FPGA uses XC5VLX50T produced by Xilinx. The image size (U, V) was 512×512 pixels, and photography was performed at a frame rate of 2000 fps.

V. EXPERIMENT

An experiment was performed to verify that the position/attitude of an object \mathbf{P}_o can be controlled by this manipulator using the control law described in Chapter III. The desired values of the position/attitude of the object were given as follows at intervals of 10 s: $\mathbf{P}_d = [x_d \text{ [mm]}, y_d \text{ [mm]}, \theta_d \text{ [deg]}] = [0, 0, -45], [7, 7, 0], [-7, 7, 45], [-7, -7, 90], [7, -7, 135], [7, 7, 180]$. The position/attitude of the object \mathbf{P}_o measured by the high speed camera is shown by the solid

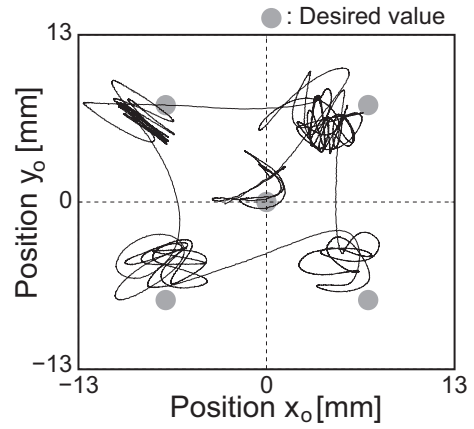


Fig. 14. Path of object during experiment

lines in Fig. 13. The dotted lines show the desired values \mathbf{P}_d . The path of the object on x - y plane after 3 s is shown in Fig. 14. It can be understood that the position/attitude of the object \mathbf{P}_o can be controlled to the desired position/attitude \mathbf{P}_d .

VI. CONCLUSION

A manipulator which enables noncontact control of the position/attitude of an object on a plane by manipulating a fluid field was proposed. The composition of the manipulator was described. The manipulator comprises 2 boards with grid pattern arrangements of holes and a parallel link robot which is capable of translational motion with 2 degrees of freedom and rotational motion with 1 degree of freedom in a plane. The principle of operation was described, and a control method was proposed. An experiment was performed, demonstrating that the position/attitude of an object can be controlled using a prototype of the manipulator.

REFERENCES

- [1] S. Iwaki, Japan patent 3999631, 2007.
- [2] T. Yamamoto, T. Takaki and I. Ishii, "Non-contact manipulation on flat plate using air-jet streams," in Proc. 27th annual conf. robot. society of Japan, 1K1-07, 2009.
- [3] S. Iwaki, H. Morimasa, T. Noritsugu and M. Kobayashi, "Contactless manipulation of an object on a plane surface using multiple air jets," in Proc. IEEE Int. Conf. Robot. Autom., Shanghai, May 2011, pp. 3257 - 3262.
- [4] A. Becker, R. Sandheinrich and T. Bretl, "Automated manipulation of spherical objects in three dimensions using a gimbaled air jet," in Proc. IEEE/RSJ Int. Conf. Intell. Robots Syst., St. Louis, MO, Oct 2009, pp. 781 - 786.
- [5] D. Biegelsen, A. Berlin, P. Cheung, M. Fromherz, and D. Goldberg, "Airejet paper mover," in SPIE Int. Symposium on Micromachining and Microfabrication, 4176/11, 2000.
- [6] J. N. Reed and S. J. Miles, "High-speed conveyor junction based on an air-jet floatation technique," Mechatronics, Vol. 14, No. 6, pp. 685-699, 1996.
- [7] S. Davis, J. Gray, and D. G. Caldwell, "An end effector based on the bernoulli principle for handling sliced fruit and vegetables," Robotics and Computer-Integrated Manufacturing, Vol. 24, No. 1, pp. 249-257, 2008.
- [8] S. Yano et al., Japan patent disclosure 2012-10633, 2012.
- [9] Y. Suzuki, M. Kobayashi, Y. Shimada, A. Nakayama and S. Iwaki, "Untethered force feedback interface that uses air jets," in Proc. Int. conf. computer graphics and interactive techniques, LA, 2004.